The serine palmitoyltransferase from Sphingomonas wittichii RW1

Manuscript received: 16/03/2010; Accepted: 22/04/2010; Article published: 23/06/2010

The serine palmitoyltransferase from *Sphingomonas wittichii* RW1: An interesting link to an unusual acyl carrier protein**

Marine C. C. Raman,[1] Kenneth A. Johnson,[2] David J. Clarke,[1] James H. Naismith,[2] Dominic J. Campopiano[1,*]

[1]EaStCHEM, School of Chemistry, Joseph Black Building, University of Edinburgh, West Mains Road, Edinburgh, EH9 3JJ, UK.

[2]Centre for Biomolecular Sciences, Scottish Structural Proteomics Facility, The University of St Andrews, Fife, KY16 9ST, Scotland, UK.

[*]Corresponding author; e-mail: Dominic.Campopiano@ed.ac.uk

[**]MCCR is funded by an EaStChem PhD studentship. The SSPF is funded by a BBSRC grant (BBS/B/14434). DJ Clarke and the high resolution mass spectrometry centre is funded by the EPSRC (EP/C543289/1) awarded to Dr. Pat Langridge-Smith and colleagues. We thank Dr. Jonathan Lowther (University of Edinburgh) and Dr. Alan Brown (University of Exeter) for helpful discussions.

Supporting information:
Additional Supporting Information may be found in the online version of this article. See http://dx.doi.org/10.1002/bip.21482

Keywords:
sphingolipids; Sphingomonas; serine palmitoyltransferase; pyridoxal phosphate;acyl carrier protein

Abstract

Serine palmitoyltransferase catalyses the first step in the de novo biosynthesis of sphingolipids. It uses a decarboxylative Claisen-like condensation reaction to couple L-serine with palmitoyl-CoA to generate a long chain base product, 3- ketodihydrosphingosine. Sphingolipids are produced by mammals, plants, yeast and some bacteria and we have exploited the complete genome sequence of *Sphingomonas wittichii* to begin a complete analysis of bacterial sphingolipid biosynthesis. Here we describe the enzymatic characterisation of the SPT from this organism and present its high resolution x-ray structure. Moreover, we identified an open reading frame with high sequence homology to acyl-carrier proteins (ACPs) that are common to fatty acid biosynthetic pathways. This small protein was co-expressed with the SPT and we isolated and characterised the apo- and holo-forms of the ACP. Our studies suggest a link between fatty acid and sphingolipid metabolism.

Introduction

Sphingolipids (SLs) are essential structural components of eukaryotic membranes and more recently they have been found to play important roles in cell signalling, inflammation and apoptosis.[1-4] They are also found in various microbial species such as yeast and fungi, as well as bacteria such as Sphingomonas. The early steps in SL biosynthesis appear to be conserved in all species studies to date; the first reaction in the pathway is catalysed by the PLP-dependent enzyme serine palmitoyltransferase (SPT). SPT produces 3-ketodihydrosphingosine by a Claisen-like condensation of L-serine and palmitoyl-CoA (Figure 1). SPT belongs to the α-oxoamine synthase (AOS)[5] family which contains three other well characterized members: 8-amino-7-oxononanoate synthase (AONS)[6,7] 5-aminolevulinate synthase (ALAS),[8-10] and 2-amino-3-ketobutyrate-CoA ligase (KBL).[11,12] Together they catalyse similar chemical reactions but have specificity for their respective amino acid and fatty acid CoA thioester substrates.

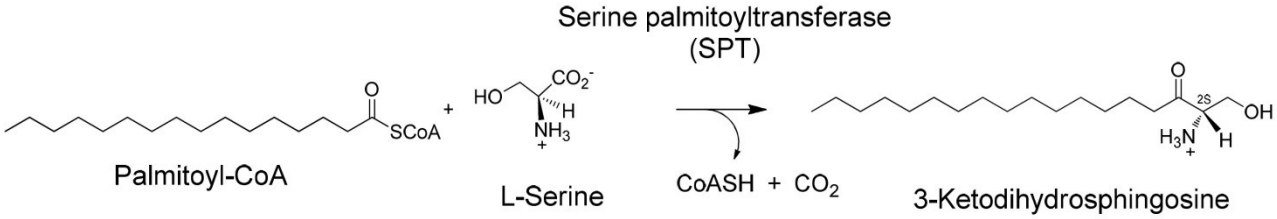

Figure 1. (a) Reaction catalysed by SPT.

Genes encoding SPT have been identified in numerous organisms but the species-specific traits of each enzyme have only emerged in recent years.[13] In humans, SPT is a heterodimeric, membrane-bound enzyme encoded by two homologous genes making its isolation in a catalytically active form extremely challenging.[14] Recent evidence suggests that the human enzyme is even more complex with the identification of two small subunits that activate in vitro SPT activity ~100 fold.[15] Insight into the structure and mechanism of SPT has been obtained from studies of a cytoplasmic, water-soluble, homodimer that was isolated from S*phingomonas paucimobilis*.[16] The interaction between this SPT and various substrates and inhibitors have also been explored.[17-19] Our group solved the first SPT structure, that of the PLP-bound, holo-form of *S. paucimobilis* that brought to light important catalytic residues and substrate specificity.[20] This also allowed a model of the human heterodimeric enzyme to be built to probe residues involved in human neurological disorders such as hereditary autonomic neuropathy type I (HSAN1). More recently, we captured the PLP:L-ser external aldimine complex which provided insight into how this key intermediate is stabilised.[21] Recently, Ikushiro *et al.* reported the structure of the holo- and external aldimine forms of SPT from the bacterium *Sphingobacterium multivorum* showing some differences with the *S. paucimobilis* SPT.[22]

As well as detailed studies on the individual enzymes involved in SL and lipid synthesis and metabolism, increasing effort has also been placed on expanding our knowledge of the structures and functions of all lipids within an organism, the field of "lipidomics".[23] Reports of the lipid content of mammals, plants and microbes have begun to appear and it is important to investigate interesting model organisms. Here, we describe our work on *Sphingomonas wittichii* RW1, a strictly aerobic Gram negative bacterium that produces both glucuronosyl and galacturonosyl ceramidetypes of SLs.[24] This is also an environmentally useful organism since it metabolises toxic pollutants such as dioxin.[25] The genome sequence of *S. wittichii* RW1 was recently completed and this stimulated our interest in using this organism as a good model for bacterial SL biosynthesis. We identified the gene encoding *S. wittichii* SPT using the amino acid sequence of the SPT from *S. paucimobilis*. Curiously, upstream from SPT, we found a small gene product that showed high sequence homology to fatty acid synthase (FAS) type II acyl carrier proteins (ACPs) (supplementary Figure 1). ACPs are small (~10 kDa), acidic proteins that play essential roles in the biosynthesis of fatty acids and other important natural products including polyketides.[26,27] ACPs are expressed in an apo-form and then post-translationally modified to their 4'- phosphopantetheine (4'-PP, holo-form using CoASH by an ACP-synthase (ACPS also known as a phosphopantetheinyl transferase, PPTase).[28] The fatty acid is built up step-bystep by enzymes within the multi-subunit FAS complex whilst attached to the ACP as a thioester.[26] ACPs have also been shown to be key components of polyketide synthases (PKS) and their peptidyl carrier protein (PCP) homologs also carry out essential roles in nonribosomal peptide synthases (NRPSs).[29] The carrier protein must interact with each of the enzymes within each complex and the exact details of these protein-protein interactions are the subject of current research.[30]

The discovery that the *S. wittichi* ACP and SPT genes are encoded by consecutive open reading frames (ORFs) on the genome suggest a possible direct link between fatty acid and sphingolipid biosynthesis. In this study, we report the structural and functional characterisation of *S. wittichii* SPT. We have also isolated and purified the linked apo-ACP and have successfully converted it into the holo-form. Sequence analysis, coupled with chemical and molecular modelling, suggest that it is an unusual apo-ACP. Our work provides the platform for future studies of bacterial sphingolipid biosynthesis.

Materials and methods

Strains, DNA and expression plasmids

The *S. wittichii* RW1 strain was a kind gift from Dr. Rolf Halden, John Hopkins University, USA. The complete genome sequence is available (http://img.jgi.doe.gov). The plasmids encoding the *Streptomyces coelicolor* ACPS (pET15b-ACPS) and *Bacillus subtilis* Sfp (pET28a/Sfp) were generous gifts from Dr. Matt Crump (University of Bristol) and Prof. Jason Micklefield (University of Manchester) respectively. The synthetic DNA construct (encoding *Streptomyces verticillus* SVP) was purchased from Mr. Gene, Regensburg, Germany.

Molecular biology reagents, chemicals and chromatography media

Plasmids (pET) and *Escherichia coli* chemically-competent cells BL21 (DE3), HMS174 (DE3) were purchased from Novagen. PCR products were cloned using the pGEM-T Easy cloning kit from Progema. Taq Polymerase Beads were from GE Healthcare. Plasmid and chromosomal DNA isolation kits were from Qiagen and used as per manufacturers' instructions. All buffers and chemical reagents were from Sigma. Palmitoyl-CoA was from Avanti Polar Lipids and [U-14C]L-serine (specific activity 1.85 MBq/ml) was from GE Healthcare. The decanoyl-CoA (10:0), lauroyl-CoA (12:0), myristoyl-CoA (14:0), stearoyl-CoA (18:0), and arachidoyl-CoA (20:0) were from Sigma. Oligonucleotide primers were purchased from SigmaGenosys. PEG 3350 was from Fluka. All chromatography columns (Ni-sepharose, gel filtration) were from GE Healthcare.

Gene Cloning

Using the Sphingomonas gene sequence (Supplementary Figure 2) four PCR products that amplified the genes encoding ACP-SPT together, ACP alone, SPT alone and ACPS were amplified using purified genomic DNA from *S. wittichii* strain RW1 as a template and the following primers:

(ACP-SPT and ACP forward BspHI)

5’-CATGTCATGAGCAGCAGAGAAGACATCTTCACC-3’

(ACP-SPT reverse HindIII)

5’-GGAAAAGCTTGGGGATTACTCCCGTGGCGCGCC-3’

(ACP reverse HindIII)

5’-AAGCTTGGAGAGGAGGTCGGCCACC-3’

(SPT forward NcoI)

5’-GGCTGACCCCATGGCCGACCTCCT-3’

(SPT reverse HindIII)

5’-TGCGGCCGCAAGCTTGGGGATTAC-3’

(ACPS forward NdeI)

5’-AGCGGGGAACCCATATGATCATCGGCATC-3’

(ACPS reverse XhoI)

5’-ATCCCCCTCGAGCAGCGGGCGCGCATACA-3’

These primers introduce appropriate restriction enzyme sites (underlined) for subsequent cloning in the *E. coli* expression plasmids; pET-28a (for ACP-SPT, ACP and SPT), pET-22b (for ACPS) designed to include a His6 tag at the C-terminus of the recombinant SPT and ACPS proteins.

The predicted sequences of the *S. wittichii* gene products (or open reading frames, ORFs) are annotated in the whole genome sequence (http://genome.jgipsf. org/sphwi/sphwi.annotation.html). This suggested that the “Swit_3900” ORF encoded an “8-amino-7-oxononanoate synthase” of 400 amino acids with high sequence homology to SPT. Sequence analysis also suggest that this ORF was translated from a GTG start codon, 10 amino downstream from a possible alternative Met start codon. Consequently, the SPT expressing clone was designed in order to produce the “isolated” SPT sequence and allow determination of the sequence of the translated protein.

The gene encoding the promiscuous phosphopantetheinyl transferase (PPTase also known as ACPS) from *Streptomyces verticillus* ATCC15003 “Svp” was generated by a commercial company (Mr. Gene, Germany)

using the sequence described in Sanchez *et al.*[31] The synthetic gene contained the restriction site *Nco*I and *Xho*I in order to clone the Svp gene in pET-22b and obtain a His6 Tag at the C-terminus to enable purification by immobilised metal affinitychromatography (IMAC) on nickel resin.

Protein Expression and Purification

Except where specified protein expression was carried out in *E. coli* BL21 (DE3) host cells transformed with the appropriate pET plasmid and grown in the appropriate selective antibiotic (ampicillin at 100 μg/ml or kanamycin at 30 μg/ml). To coexpress *S. wittichii* ACP and SPT, cells transformed with the appropriate plasmid (pET-28a/ACP_SPT SW) were cultured in 2YT media (16 g/l Bacto-tryptone, 10 g/l Bacto-yeast extract, 5 g/l sodium chloride (pH 7.5)) including the appropriate antibiotic at 30°C for 3-5 hrs in the presence of 0.1 m*M* IPTG to induce protein expression. To express the *S. verticillus* Svp protein, the expressing plasmid was used to transform HMS 174 (DE3) cells which were grown at 30°C for no longer than 3 hours to avoid any mis-folding and inactivation of the enzyme. It is important to note that it was not possible to express the *S. wittichii* ACP alone, thus we co-expressed the ACP with SPT from the T7 promoter on the pET plasmid. Induced cells were harvested (Sorvall RC5B centrifuge) by centrifugation at 3500 rpm for 20 min at 4°C.

For the isolation of all recombinant proteins, the cell pellet was resuspended in 20 m*M* potassium phosphate buffer (pH 7.5) containing one EDTA-free protease tablet (Roche) before being disrupted by sonication (Soniprep 150) for 15 cycles (30 s on, 30 s off) on ice. The cell debris was removed by centrifugation at 16,000 rpm for 30 min at 4°C and the supernatant cell-free extract was filtered (0.45 μ m syringe filter), before being loaded onto the appropriate chromatography column. All chromatography steps were carried out at 4°C using an ATKA (GE Healthcare) to control flow rates and salt gradients.

Each of the poly-histidine tagged recombinant proteins, *S. wittichii* SPT, *B. subtilis* Sfp and *S. coelicolor* ACPS were purified according to the previously described methods [21,32,33]. Cell free extracts containing recombinant *S. wittichii* ACP protein in 20m*M* potassium phosphate buffer (pH 7.5) were loaded onto a HiLoad Q-sepharose anion exchange column (50 ml, GE Healthcare) preequilibrated with 20 m*M* potassium phosphate buffer (pH 7.5). The ACP protein was eluted with a linear salt gradient (0-1.0 M KCl) over 20 column volumes (1 litre). Fractions containing ACP were identified by SDS-PAGE analysis, pooled and loaded onto a calibrated HiLoad 16/60 Superdex 75 prep grade (120 mL) size exclusion column. Elution was carried out in 20 m*M* potassium phosphate buffer (pH 7.5), 150 m*M* NaCl.

The his-tagged *S. wittichii* ACPS in 20 m*M* potassium phosphate buffer (pH 7.5), 150 m*M* NaCl, 10% glycerol (v/v) and 20 m*M* imidazole was loaded onto a HiTrap Chelating HP column pre-equilibrated with the same buffer. The protein was eluted with a linear gradient [20 m*M* to 500 m*M* imidazole] over 10 column

volumes. Fractions containing ACPS were pooled and loaded onto a previously calibrated HiLoadTM 16/60 SuperdexTM 75 prep grade (120 mL) size exclusion column. The pure protein was eluted at a flow rate of 1.2 ml/min in 20 m*M* potassium phosphate buffer (pH 7.5), 150 m*M* NaCl, 10 % Glycerol. The *S. verticillus* Svp protein was purified following the same protocol that was used for *S. wittichii* ACPS isolation but the purification buffer did not contain any glycerol.

For storage, the enzyme solutions were brought to a final concentration of 20% glycerol (v/v) (*S. wittichii* SPT, *S. wittichii* ACP, *S. coelicolor* ACPS, *B. subtilis* Svp) or 40% glycerol (*Streptomyces verticillus* Svp and *S. wittichii* ACPS*)* and stored at -80 °C until use.

Protein identity and integrity were confirmed by routine high pressure liquid chromatography electrospray mass spectrometry (HPLC-ESI MS) on a MicroMass Platform II quadrupole mass spectrometer equipped with an electrospray ion source. The experimentally determined masses of each recombinant protein were within 0.1% of the predicted masses based on their amino acid sequences.

Determination of the "isolated" *S. wittichii* SPT N-terminus

The ORF annotated as "Swit_3900" in the *S. wittichii* genome sequence is predicted to encode a "8-amino-7-oxononanoate synthase, AONS". The translated protein is predicted to contain 400 amino acids and a theoretical mass of 43095 Da. To determine the actual size of the ORF we cloned ORFs "Swit_3899" and "Swit_3900" together in a pET plasmid with a single T7 promoter and a six histidine tag at the C-terminal end of ORF Swit_3900. Expression of both genes was induced with IPTG and the Swit_3900- encoded protein was purified using standard IMAC procedure. After LC ESI-MS analysis, the mass of the purified recombinant protein was 44,515 Da which is in good agreement with a sequence containing 412 amino acids that has lost the N-terminal methioine residues and includes the C-terminal KLAAALEHHHHHH affinity fusion tag. Therefore, the purified Swit_3900 protein, hereafter named SPT SW, resembles a Nterminally truncated SPT SP (lacking 20 amino acids).

Spectroscopic Measurements and Determination of Dissociation Constants

All UV-visible spectra were recorded on a Cary 50 UV-visible spectrophotometer (Varian) analyzed using Cary WinUV software (Varian). We used the protocol previously described in Raman *et al*., to characterise the spectroscopic properties of the recombinant *S. wittichii* SPT.21 Briefly, the SPT was converted to its external aldimine (holo-) form by dialysis against freshly-prepared buffer containing 20 m*M* potassium phosphate buffer (pH 7.5), 150 m*M* NaCl, 25 μM PLP for 1 hour at 4 °C. We removed excess PLP by passage through a PD- 10 column (GE Healthcare) eluting with the same buffer without PLP. The protein was

concentrated to 10-20 mg/ml using a VivaSpin 30 kDa cut-off ultrafiltration spin filter. The dissociation constant for L-serine (*Kd*) was determined spectroscopically by monitoring the changes (at 425nm) upon incubation of the protein with increasing concentration of L-ser (0-80 m*M*). Data were fitted to a hyperbolic saturation curve using Sigma Plot software as described in Raman et al.[21]

Assay of Recombinant SPT Activity

We used methods previously described in Raman *et al*.,[21] to determine the catalytic activity of *S. wittichii* SPT with a range of substrates. Product formation was monitored by following production of [14C] KDS from [14C] L-serine using thin layer chromatography and autoradiography. SPT activity was also monitored continuously by measuring the release of CoASH by reaction with 5,5'-dithiobis-2-nitrobenzoic acid (DTNB) at 412 nm.

Structural Biology

The SPT protein was screened for suitable crystallization conditions at the Scottish Structural Proteomics Facility. The proteins were dialyzed in the presence of excess PLP to ensure complete reloading prior to crystallization. The screens were built on a Hamilton Microstar liquid-handling robot controlled by Rhombix system software (Thermo).

The *S. wittichii* SPT was crystallized at 20 mg/ml in 10 m*M* Tris (pH 7.5), 150 m*M* NaCl, 25 μ M PLP using 30% PEG monomethylether (MME) 2000, 0.1M KSCN, (NEXTAL JCSG+ screen condition 81). Crystals used for data collection were soaked for a few minutes in a solution of 27% PEG MME 2000, 0.22M KSCN, 18% PEG400 plus 1–2 m*M* PLP.

The crystal was mounted in a cryoloop (Molecular Dimensions) and frozen by plunging it into liquid nitrogen and carried in a dry cryogenic Dewar to the European Synchrotron Radiation Facility (Grenoble, France) for data collection. Multiple crystals were screened at beam line BM14 .The data sets were collected at 100 K to 2.1 Å using beam line 14 (supplementary Table 1). The data for *S. wittichii* SPT were processed with Mosflm and scaled with Scala from the CCP4 suite of programs.[34,35] The density revealed that the PLP was covalently bound to Lys245 confirming that we had obtained the internal aldimine, holo-form of the protein. The SPT model was refined using Refmac534 and manually adjusted, including the addition of water molecules with WinCoot.[36] Data and structure files have been deposited in the Protein Data Bank (PDB ID code 2xBU).

Conversion of *S. wittichii* apo-ACP to holo-ACP and acyl-ACP.

The protocol used to modify the *S. wititchii* apo-ACP with the different phophopantetheinyl transferases (PPTases) was modified from previously described methods.[31-33]

For brevity, the protocol is described using the generic name, "PPTase" that refers to each of the recombinant ACPS enzymes used; *S. coelicolor* ACPS, *B. subtilis* Sfp, *S. verticillus* Svp and *S. wittichii* ACPS.

A final enzyme concentration of 60 μM apo-ACP in reaction buffer (see below) was incubated with 1 μM PPTase, 1 m*M* MgCl2 and a range of concentrations of CoASH/acyl-CoA (250 μM to 1 m*M*) in a final volume of 250 μL. The reaction was incubated at 37 °C overnight and then analysed by LC ESI-MS to determine the extent of modification of the apo-ACP.

For each PPTase a different reaction buffer was used. For *S. coelicolor* ACPS and *S. verticillus* Svp, 50 m*M* Tris buffer, pH 7.8 was used. For *B. subtilis* Sfp we carried out the reaction in 75 m*M* MES buffer at pH 6.0 and for *S. wittichii* ACPS this was performed in 20 m*M* potassium phosphate buffer (pH 7.5). 5 mM DTT was added to the reaction mixture when using free CoASH as a substrate.

It is important to note that MgCl2 concentrations of > 1m*M* could not be used for reactions containing acyl-CoAs as this caused precipitation of these substrates.

High Resolution LC-FT-ICR Mass Spectrometry analysis

For high resolution mass spectrometry (LC-FT-ICR MS), an Ultimate 3000 HPLC system (Dionex Corporation, Sunnyvale, CA), equipped with a monolithic PS-DVB (500 μM x 5 mm) analytical column (Dionex Corporation), was used. MS data was acquired on a Bruker 12 Tesla Apex Qe FTICR (Bruker Daltonics, Billerica, MA) equipped with an electrospray ionization source. Desolvated ions were transmitted to a 6 cm Infinity cell® penning trap. Trapped ions were excited (frequency chirp 48-500 kHZ at 100 steps of 25 μs) and detected between *m/z* 600 and 2000 for 0.5 s to yield a broadband 512 Kword time-domain data. Fast Fourier Transforms and subsequent analyses were performed using DataAnalysis (Bruker Daltonics) software. Multiple charge states could be observed in this way for each of the major species.

Isotopic Fitting. Isotope distributions of specific charge states were predicted using IsotopePattern software (Bruker Daltonics) from theoretical empirical formulae. These were overlaid upon the recorded experimental data as scatter plots, with the theoretical apex of each isotope peak designated by a circle.

Top-Down Fragmentation. Top-down fragmentation was performed on the 12T Qh- FT-ICR. Two specific ions, m/z 1521 and 1304, were sequentially isolated using the mass resolving quadrupole, and MS/MS was

performed using collision induced dissociation (CID). For CID, the collision voltage was typically set between 20-35V. Fragmentation data was the sum of 200 acquisitions and data analyses were performed using DataAnalysis (Bruker Daltonics). The SNAP 2.0 algorithm was used for automated peak picking. The resulting top-down fragment mass lists were combined and searched against the primary sequence of ACP using Prosight-PTM software.37 Mass error tolerances were set for all searches at 10 ppm.

Results and discussion

Purification and Characterisation of *S. wittichii* SPT

Using BLAST analysis we searched the annotated genome of the sphingolipidproducing organism *S. wittichii* RW1 for the gene encoding a homologue of *S. paucimobilis* SPT. We identified a hit ORF with 70% sequence identity that was annotated as "Swit_3900". It had been labelled as an AONS catalysing the first step in biotin biosynthesis (condensation of L-alanine and pimeloyl-CoA to generate 8-amino-7-oxononanoate, AON6) since there is highly conserved sequence homology between members of the AOS family. We also noted that just upstream of "Swit_3900" another small gene, "Swit_3899" had been annotated with "unknown function". Upon sequence analysis of this translated 80 aa protein we found a conserved phosphopantetheinylation sequence motif (DSLT) characteristic of acyl carrier proteins (supplementary Figures 1 and 2).29,38 The conserved serine residue is post-translationally modified using CoASH as a substrate to convert the apo-ACP into the holo-ACP form containing a 4'-phosphopantethiene (4'-PP) prosthetic arm.[28] Further sequence analysis of the two genes suggested the presence of a typical bacterial promoter upstream of the predicted ACP gene and ribosome binding sites (RBSs) before the putative ACP gene (supplementary Figure 2). A consensus RBS could not be detected for the SPT gene.

To explore the structure and function of this pair of proteins we cloned both genes into a pET expression plasmid to determine if both genes could be transcribed from the strong plasmid-encoded T7 promoter. We also fused a six-histidine tag at the C-terminal end of the putative SPT to enable facile purification by IMAC since this tagging strategy worked well with our previous *S. paucimobilis* SPT. We induced transcription from the T7 promoter of the expression plasmid pET-28a/ACP_SPT SW using IPTG and we analysed the expressed protein products by SDS-PAGE (Supplementary Figure 1b). Two clearly overexpressed bands were observed at ~8-10 kDa and ~45 kDa corresponding to the ACP and SPT gene products respectively. This result confirmed that both genes could be expressed from a single external promoter and suggested that the SPT product was translated from a RBS on the RNA transcript.

A large scale culture was carried out with these expressing cells, a cell-free extract was prepared in the presence of PLP (25 μM) and then subjected to IMAC to isolate the Histagged putative SPT SW. Upon elution with imidazole we obtained fractions highly enriched in a single 42 kDa protein which was further

purified using size exclusion chromatography. The protein eluted as a dimer and its UV-vis spectrum showed characteristic absorbance maxima at 340 nm and 425 nm which correspond to the enolimine and ketoenamine forms of the PLP-bound enzyme (Supplementary Figure 3). By measuring the change in absorbance at the ketoenaminespecific wavelength at 425nm, the dissociation constant for L-serine (*Kd* L-Ser) was found to be 0.8 m*M* which is in the same range as the value (1.1 m*M*) obtained for the *S. paucimobilis* SPT (Table 1).[18,21]

Table 1. Kinetic Parameters for the Purified SPT ***S. wittichii*** and ***S. paucimobilis***

Enzyme	k_{cat} x 10^3 (s^{-1})	K_m^{Ser} (mM)	K_m^{PCoA} (µM)	k_{cat}/K_m^{Ser} ($M^{-1}s^{-1}$)	k_{cat}/K_m^{PCoA} ($M^{-1}s^{-1}$)	K_d^{Ser} (mM)
SPT *S. wittichii*	68.7 +/- 1.5	0.78 +/- 0.10	23.4 +/- 4.5	88.1	2,936	0.80 +/- 0.1
SPT *S.paucimobilis*	1150.0 +/- 30.0	1.40 +/- 0.10	35.4 ± 2.0	821.4	32,486	1.1 +/- 0.1

We noted that during isolation of the His-tagged SPT SW by IMAC, the putative ACP protein did not bind to the column, so this unbound fraction was used for the isolation of the ACP by ion-exchange chromatography (see below).

SPT activity and kinetics

We measured KDS production catalysed by the SPT SW with [14C] L-serine and palmitoyl-CoA using the method described previously (Supplementary Figure 3b).39 We also used a continuous, spectroscopic DTNBlinked assay that detects formation of CoASH to determine kinetic parameters of the enzyme. The SPT SW bound L-serine and palmitoyl- CoA with *Km* values of 0.78 m*M* and 23.4 μ M, respectively (Table 1). The enzyme turned over with a *k*cat of 0.069 s-1 and a catalytic efficiency (*k*cat/*Km* **Ser**) of 88.1 M-1 s-1 for Lserine. A comparison of the kinetics of the SPTs from *S. wittichii* and *S. paucimobilis* revealed that both enzymes display similar binding affinities for both substrates but that the SPT SW had a much lower turn over and efficiency (~17 fold for *k*cat; and 9 and 11 fold for *k*cat/ *Km* for L-ser and palmitoyl-CoA respectively) compared with the SPT SP.

The acyl-CoA chain length specificity of the SPT SW was also investigated. We found stearoyl-CoA (C18:0) to have the fastest turnover (*k*cat = 0.083 s-1) of all of the acyl-thioesters tested and a *Km* of 12.9 μ M (Supplementary Table 2). When comparing the *k*cat/*Km* values, stearoyl-CoA (C18:0) was also the most efficient substrate (6,416 M-1 s-1). In contrast, the decanoyl-CoA (C10:0) and lauroyl-CoA (C12:0), were the poorest substrates and accurate kinetic constants could not be determined.

These combined results suggested that although the SPTs from these different strains displayed high sequence identity and similar substrate binding specificities there could be subtle differences that would lead to differences in turnover rates. It appeared that the SPT from both Sphingomonas strains bound L-serine with the same affinity (similar *Kd* values) and similar *Km* values for CoASH ester substrates but there were a large differences in catalytic rates. The presence of a putative ACP that co-expressed with the SPT suggested that instead of using palmitoyl-CoA as a thioester substrate, the *S. wittichii* SPT could possibly use an acyl-ACP thioester substrate.

High resolution crystal structure of *S. wittichii* SPT

S. wittichii SPT crystallised as a dimer in the asymmetric unit, in contrast to the *S. paucimobilis* SPT where the dimer is generated by crystal symmetry (Figure 2a).[20-22] However, both the dimer and monomer structures are similar (with a few differences) between the Sphingomonas strains, root mean square (rms) deviation for the dimer is 0.65 Å (796 C alpha backbone) and 0.61 for the monomer (398 C alpha backbone). In our previous SPT SP structure it was also not possible to model the N-terminal 22 amino acids and in both SPTs the C-terminal hexahistidine affinity tags were not visible. The SPT SW is shorter at the N-terminus compared to the SPT SP and therefore the SPT SW model contains 398 of the 412 amino-acids from Ala2 to Pro400 inclusive. The PLP cofactor is bound in both monomers in a similar way. All SPT:PLP interactions observed with the cofactor in one active site are also present in the second PLP-binding site within the dimer. The PLP cofactor forms hydrogen-bonds to the side chains of Asn118, Thr242, Thr274, the main chains of Gly114, Tyr115, Ala275 and π-stacks with His139 (Figure 2b). Overall the SPT SW and SPT SP active sites bear very close resemblance to each other (Figure 2c).

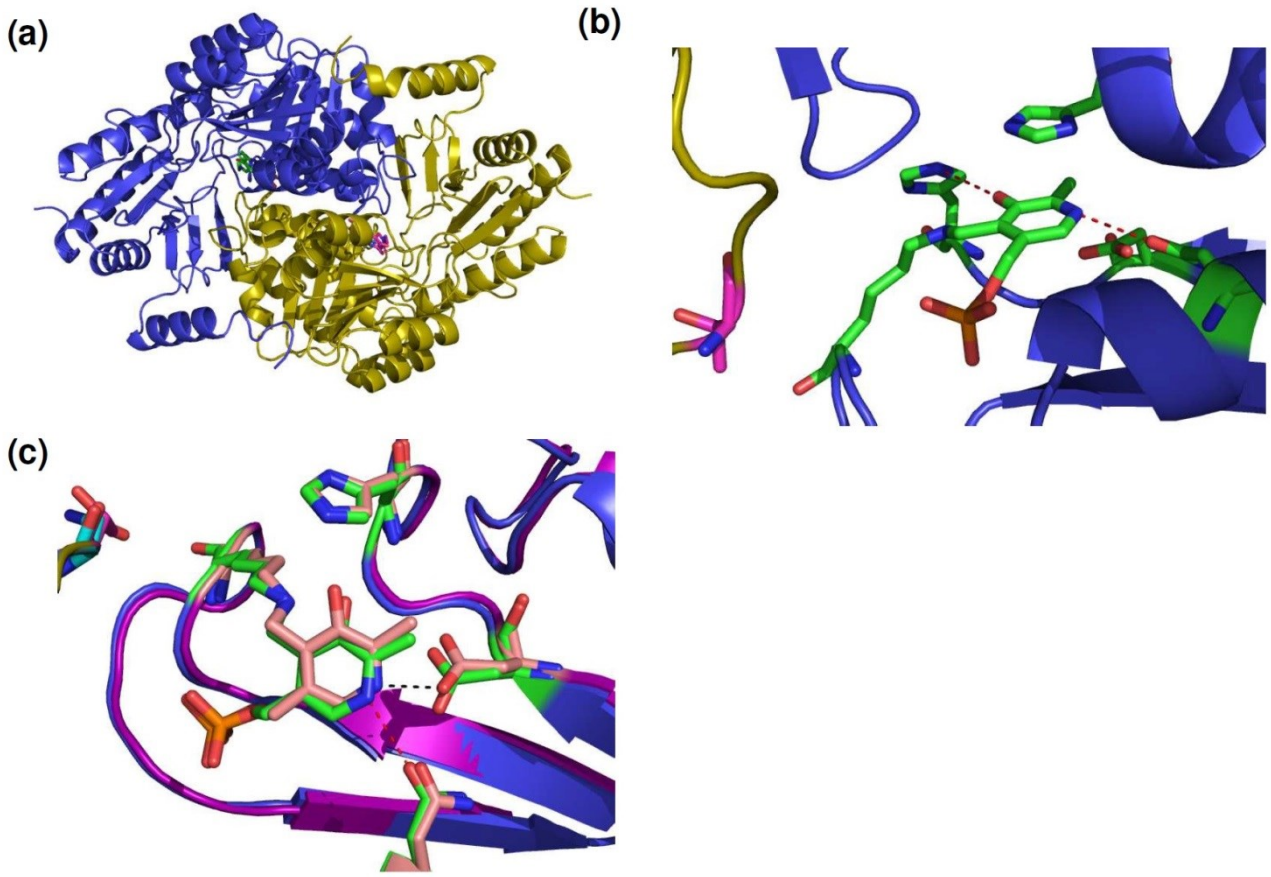

Figure 2. Structure of *Sphingomonas wittichii* SPT (a) overall structure of the SPT dimer showing one monomer in *blue* and the other in *olive*. The cofactor PLP bound to the residue Lys265 in the *blue* monomer is shown in *stick form* and is *colored green*. The equivalent residue from the *olive* monomer is colored *magenta* (b) catalytic site view showing the cofactor PLP of monomer A and the residues His139, His214 and Asn118 involved in its stabilisation. Monomer A is drawn in *blue* and monomer B is drawn in *olive*. (c) Overlay of SPT SW and SPT SP showing similar residues involved at active site. SPT SW is coloured *blue* and the PLP plus active sites residues are represented in *green*. SPT SP is coloured magenta and the PLP cofactor and the active site residue are *pink*.

Two important interactions present in *S. paucimobilis* SPT and also found in other members of the AOS family appear to be absent in the SPT SW structure. Both Asp211 and His214 appear to be too far away to form interactions to the PLP pyridine nitrogen and PLP oxygen atoms respectively, that have been observed in other structures. Both these residues are absolutely conserved among all SPTs and AOS family members and are known to stabilise and anchor the PLP in the active site. Even if these residues are too far away to interact with PLP in this crystal structure, they may be involved during catalysis in solution possibly by stabilisation of other intermediates (e.g. formation of the PLP:L-Ser external aldimine). We do note that a possible

compensatory interaction involves the sidechain of Asn118 which is closer to the pyridine nitrogen of the PLP ring than the equivalent residue (Asn138) in the SPT SP structure. In the *S. paucimobilis* SPT structure we found that an arginine residue, Arg378, played a role in anchoring the carboxylate residue of L-Ser in the PLP:L-Ser external aldimine form of the enzyme. In SPT SP the side chain of Arg378 undergoes a large conformational change from the holo- "swung-out" form to the external aldimine "swung-in" form.[21] We note that in SPT SW residue Arg358 is suggested to play this role and is in the "swung-out" position characteristic of the holo- form of the enzyme.

Other small differences can be observed between the two bacterial SPTs. In our previous study of *S. paucimobilis* SPT we used the bacterial, homodimeric enzyme to generate a model of the heterodimeric (SPT1/2) human SPT.[20] We used this model to predict the site of mutation in the human SPT1 subunit (Cys133, which is mutated to Tyr and Trp) that causes the sphingolipid metabolic disease HSAN1. Our model suggested *S. paucimobilis* SPT residue Asn100 mapped to human SPT1 residue Cys133 and this side-chain plays a role in contacting the backbone amide of the PLPbinding residue Lys265. In a recent study we probed its structural and function role by making Asn100Tyr and Asn100Trp mutant SPT SP.[21] This revealed that mutations on one SPT monomer do indeed impact on the other. In *S. wittichii* SPT the Asn100 residue is replaced by Thr80, other sequence changes place it in a hydrogen bonding environment at the interface between the two subunits. In contrast to Asn100 of SPT SP, the side-chain of Thr80 does not make a direct hydrogen bond contact with the other subunit but is immediately adjacent to PLP binding Lys245 of the neighbouring subunit (Figure 2c).

We also observed other small differences between the SPT structures from both Sphingomonas strains. The entrance to the active site that is situated at the "top" of the SPT SW protein surface is wider than that observed in *S. paucimobilis* SPT, possibly indicating the binding of a larger long-chain fatty acid substrate (e.g. acyl-ACP) instead of an acyl-CoA thioester (Supplementary Figure 4). This results from a rigid movement of the loop Pro360-Pro363 of about 2 Å. The residues within this loop are conserved between SPT SP and SPT SW, however Met366 is found in SPT SW and is replaced with Thr386 in SPT SP; whilst residue Thr356 in SPT SW is replaced by Met376 in SPT SP. As a result the methionine side chain sits in different hydrophobic pockets in both enzymes and this may be responsible for the different loop positions. These comparisons suggest that there are subtle structural differences between the bacterial SPT isoforms that could explain observed differences in their catalytic activities.

To further probe the Nature of the acyl-CoA binding site we used the structure of the recently solved enzyme CqsA from *Vibrio cholerae*, a recent addition to PLP-dependent, AOS family, which resembles SPT and AONS.[40] CqsA is involved in the biosynthesis of cholerae autoinducer-1 (CAI-1) from (S)-2- aminobutyrate and decanoyl-CoA.[41] Of particular interest, the external aldimine of the final product from the condensation of Lthreonine and decanoyl-CoA has been trapped in the active site (PDB ID code: 2WKA). Superposition of the SPT SW and *V. cholerae* CqsA structures places the acyl-CoA binding site in a long hydrophobic channel

at the interface of the two monomers of SPT SW (Figure 3a and 3b). The channel is lined by residues Leu10, Arg15, Ala17-Leu19, Thr21- Tyr27, Val341, Arg358-Pro361 from monomer A and Val84-Leu85, Leu266 and Val272 from Monomer B. Two valine residues (Val23 and Val341 from monomer A) delimit the end of the channel. We note that SPT SW has a lower chain length limit with regard to its acyl-CoA substrates and we detected no activity with substrates of C12 and below. The exact details of chain length specificity within the AOS family are still unknown but this analysis will allow us to probe the role of the residues lining this putative channel.

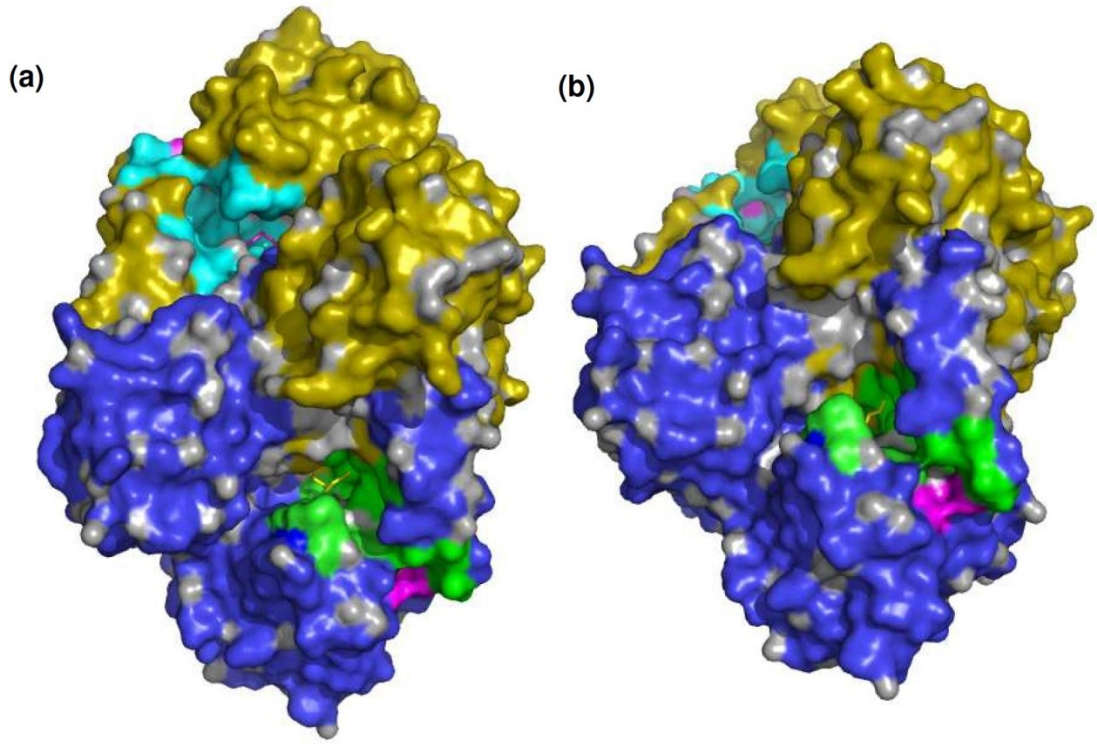

Figure 3. Surface structure of SPT showing palmitoyl-CoA binding cavity (a) View from the top (b) Top/side view. Monomer A is show in *blue* and monomer B in *olive*. The two hydrophobic cavities are coloured *cyan* and *green*. The end of each channel is delimited by two valine residues Val23 and Val341 shown in *magenta*.

Purification, Characterisation and Modification of Apo-ACP

S. wittichii ACP was co-expressed with SPT in *E. coli* and a rapid two-step purification procedure using anion exchange and size-exclusion chromatography led to the isolation of milligram quantities of the protein. We used LC ESI-MS to determine the mass of the purified protein (8784 Da) and this revealed that the ACP SW had been expressed in the apo-form (predicted mass without Met residue 8782.5 Da, Figure 4a). This suggests that the enzymes involved in post-translational modification of the Type II FAS machinery in *E. coli* do not recognise the *S. wittichii* ACP and cannot convert it to the 4'-PP holo form.

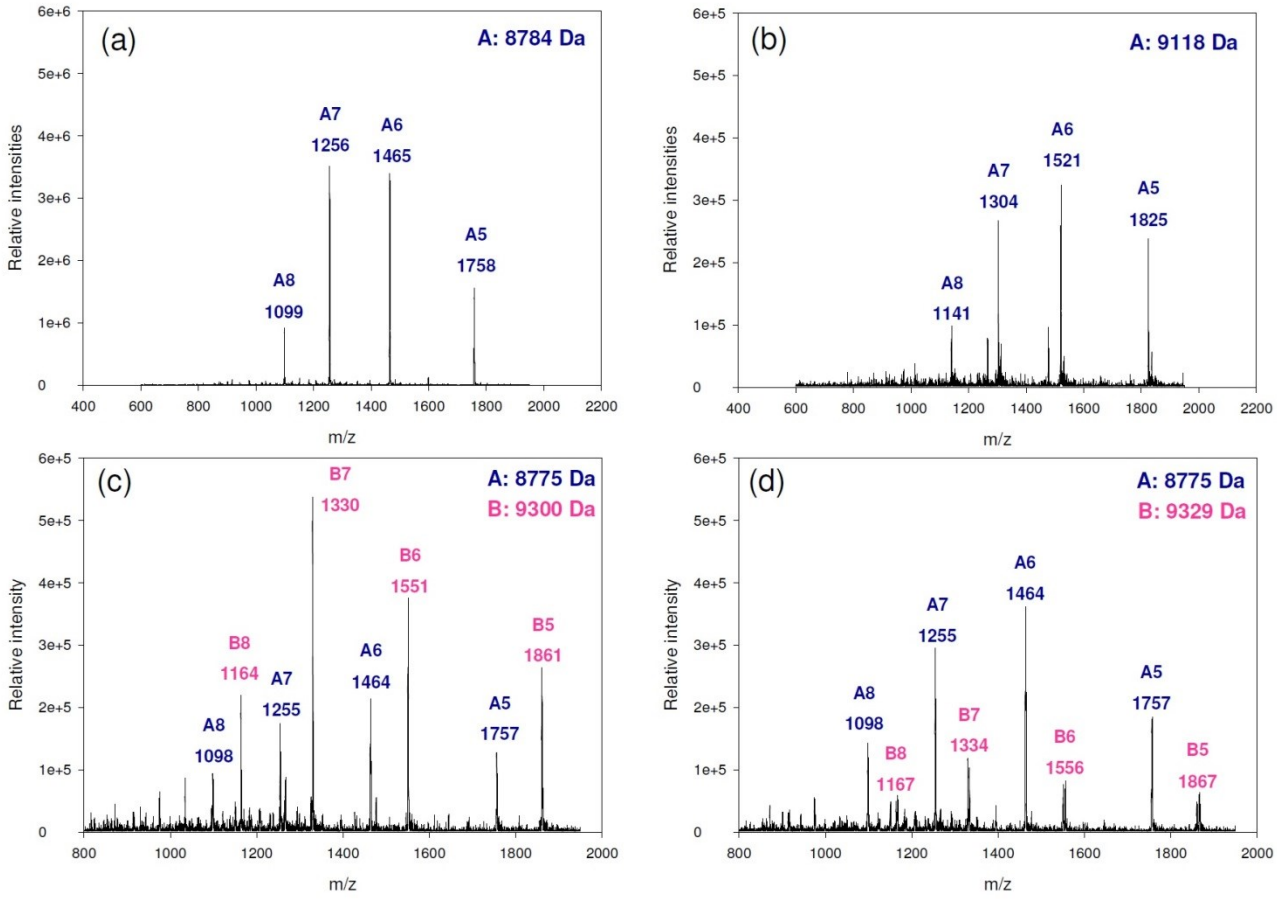

Figure 4. Mass spectrometry of ACP. Ion envelopes of (a) Apo-ACP (b) Holo-ACP (c) Lauroyl-ACP (d) Myristoyl-ACP. Apo-forms of ACP are shown in *blue*. Holo and acyl-forms are shown in *red*. The deconvoluted experimental masses based on the ion envelope are shown.

Generally, ACPs are modified by a PPTase (also known as ACPS) by the addition of the 4'-PP group and thereafter the fatty acid chain is built up step-by-step by a fatty acid synthase (FAS).[26] Individual members of the PPTase superfamily tend to display high substrate specificity and will only recognise their cognate ACP.[28] This has caused technical problems with regard to production of various natural products in recombinant hosts (and in vitro) where the ACP is not modified correctly. Some PPTases are able to catalyse the direct transfer of an acyl group to an apo-ACP using an acyl-CoA substrate, thus generating an acylated-ACP in a single step. Some of these PPTases are well known for their broad substrate recognition and inherent "promiscuity" and have been used to solve problems of production of natural products in alternative hosts.[27,31-33] Since we isolated the ACP SW in an apo- form we wished to convert it to the holo- and various acylated forms. We used CoASH to install the 4'-PP arm, as well as acyl-CoAs of varying fatty acid chain length (decanoyl C10; lauroyl C12; myristoyl C14; palmitoyl C16 and steroyl C18) in combination with a number of PPTases.

The first attempt to modify ACP SW (with CoASH and acyl-CoAs) was made with the *S. coelicolor* ACPS since it is known to have broad specificity.[33,42] Unfortunately, this did not give any positive results (data not shown) and this suggested that *S. coelicolor* ACPS does not recognise ACP SW. We next tried the broad-range ACPS *B. subtilis* Sfp and found it did successfully convert the apo-ACP into the holo-form with an increase mass of 4'- PP (experimental mass 9118 Da, Figure 4b) as well as the C10 (data not shown), C12 (mass 9300 Da, Figure 4c) and C14 (mass 9330, Figure 4d) acyl-ACP derivatives. The % conversions of apo- to the C12- and C14- modified ACPs (based on MS peak height intensities) were ~50% and ~20% respectively. We also used high resolution MS coupled with fragmentation techniques to identify the site of 4'-PP attachment on the holo-ACP SW as the Ser39 residue within the conserved motif (Supplementary Figure 5). Unfortunately, *B. subtilis* Sfp failed to transfer a palmitoyl (C16:0) or a stearoyl (C18:0) chain onto the apo-ACP SW. The transfer of the palmitoyl chain by *B. subtilis* Sfp was further explored by testing several reaction conditions (varying enzyme, substrate and co-factor concentrations as well as temperature and time) without any success (data not shown). Previous studies reported that *B. subtilis* Sfp was successfully used to modify a large number of ACPs and PCPs with various substrates but never with long chain fatty acids (≥ C16).[32,43,44]

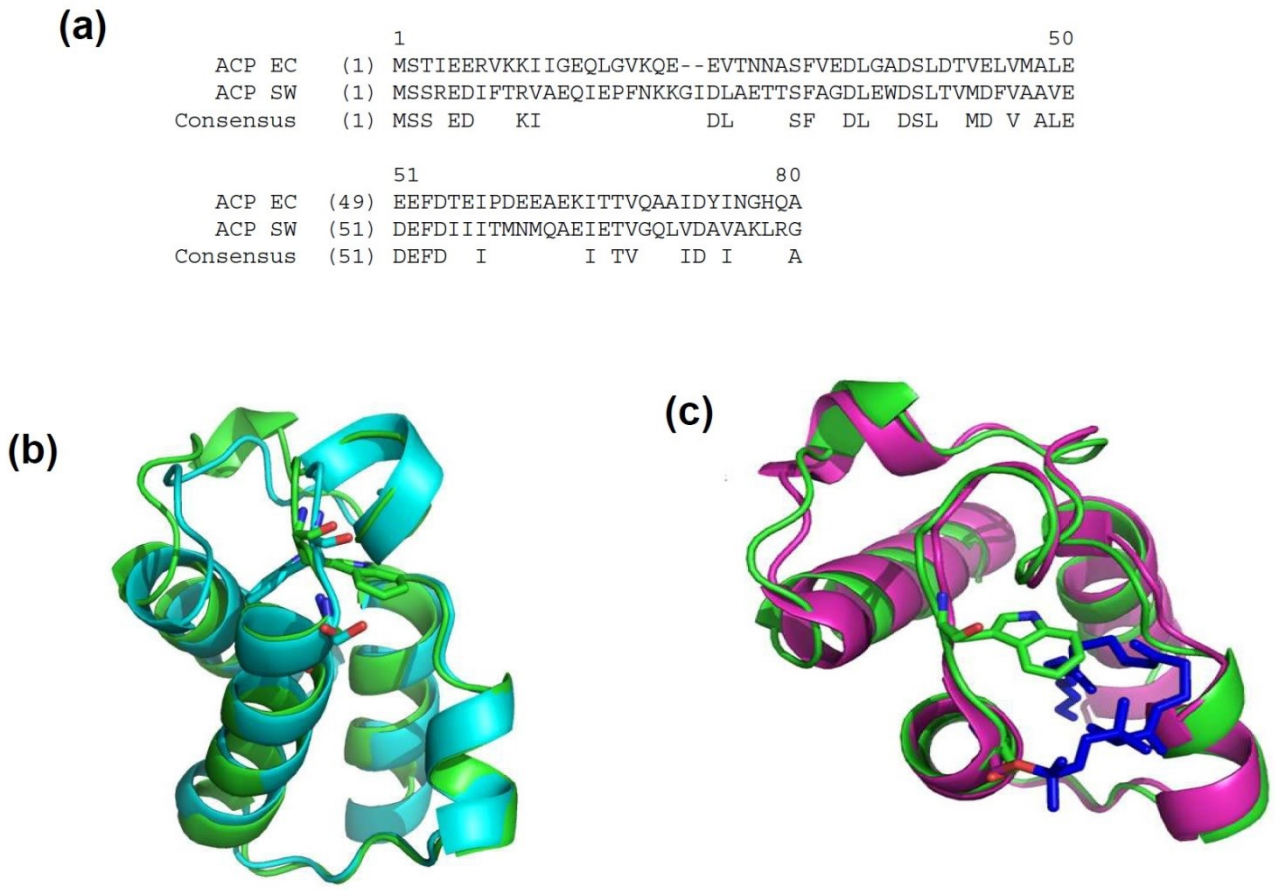

Figure 5. (a) Sequence alignments of *E. coli* and *S. wittichii* ACPs (b) 3D-Models of ACP *S. wittichii* showing superposition of Swiss and JIGSAW ACP 3D-models. The ACP Swiss-model is coloured cyan and

JIGSAW-model is coloured green. In each model, residue Trp37 is shown in stick form. (c) Superposition of the JIGSAW *S. wittichii* ACP model and *E. coli* ACP structure (PDB ID: 1LOH). The ACP SW JIGSAW-model is coloured *green* and *E. coli* structure in *magenta* with the C4 acyl group shown in stick form and coloured in *dark blue*.

Another useful promiscuous PPTase, *S. verticillus* Svp, with similar characteristics to Sfp, has been shown to have a preference for longer carbon chains.[45] It was also shown to modify both type I and type II ACPs and PCPs from either *S. verticillus* or other Streptomyces species.[31] However, although we found that *S. verticillus* Svp converted apo-ACP SW to the holo form it failed to transfer any acylthioester substrates (data not shown). Since the *S. verticillus* Svp and other PPTases are able to catalyse formation of holo-ACP SW but are not able to transfer an acyl-4'-PP group, we suggest that the problem with the long chain transfer must come from the structure of the ACP SW itself. Finally, we used sequence homology to identify the PPTase (ACPS) in the *S. wittichii* genome (ORF code Swit_3872) that enabled us to overexpress this PPTase in *E. coli*. We were able to purify the recombinant *S. wittichii* ACPS but found that in assays with apo-ACP SW this enzyme catalysed only the formation of the holo-form and provided no acyl-ACP. Similarly, co-expression of ACP SW and ACPS SW inside the same *E. coli* host provided only holo-ACP (data not shown).

In conclusion we found that *B. subtilis* Sfp was the best PPTase to act upon the apo-ACP SW. Unfortunately, we were unable to generate sufficient quantities of long chain acylated-ACP to carry out a study of its ability to act as an acyl-donor in the SPT reaction with L-serine. In a recent study on rat Type I ACP the authors also noted the tendency of the C16-acylated form of this protein to precipitate over 48 hrs.[42] We also realised through our acyl-CoA chain length kinetic analysis that SPT SW failed to accept substrates with carbon chain lengths of less than C14 (supplementary Table 2). To generate sufficient quantities of long chain acyl-ACP SW we may need to turn to a chemical, non- enzymatic procedure using N-acylimidazole derivatives and this is a target of future work.[46]

ACP structural model

Since we found the apo-ACP SW was so difficult to convert to an acylated form using promiscuous PPTases we carried out sequence analysis to identify any novel characteristics that could explain its recalcitrant nature. Protein sequence alignment revealed that ACP SW is rather unusual and does not fit perfectly into an ACP sub-family described in the literature. Its closest homologs are proteins with no published experimental data associated with them. However, it does show 26% amino acid sequence identity to *E. coli* ACP which has been characterised extensively (Figure 5a).[47] In ACP SW one particular residue stands out - a highly uncommon tryptophan residue (Trp37) positioned just before the conserved (WDSLT) 4'-PP sequence motif

(Figure 5a). Numerous ACP structures are available in the literature in both apo-, holo- and acylated forms.[29,38] Despite acting in diverse biosynthetic pathways, interacting with many different enzymes and having low overall sequence similarity, their secondary structures and overall folds are very similar.[27] For example the *E. coli* ACP is typical and displays a common fold of four α-helices. Thus, using the 3D-JIGSAW server[48-50] and Swiss-model[51-53] we were able to generate two 3D-models of ACP SW in order to gain some insight into the role of this unusual tryptophan residue (Figure 5b and 5c). The ACP SW model was based on a best fit to that of the ACP from *E. coli*.[47] This ACP was shown to be able to accommodate a growing acyl chain within a hydrophobic cavity that could expand as fatty acid synthesis proceeded. The ACP SW models adopted the typical four α-helical bundle fold. Superposition of the two models generated by the different software revealed two possible positions for the Trp37 side-chain both of which are close to the site of 4'-PP attachment (Ser39) (Figure 5b). In both models the residue is positioned on a solvent-exposed flexible loop and so one could imagine that the tryptophan could adopt both conformations. The superposition of the 3D-JIGSAW model with the C4-ACP *E. coli* structure (Figure 5c) lends weight to the attractive idea that this unusually placed tryptophan could control transfer of 4'-PP and/or long chain acyl groups. Indeed, we found that the holo-ACP SW could be generated from the apo-form by incubation with various PPTases but these structural models also provide a possible explanation for the lack of modification of the ACP SW with longer chain acyl-CoAs (>C16) in appreciable yields. It may be that the ACP SW is converted to a long chain acyl-CoA form only within *S. wittichii* as part of fatty acid synthesis. Thus, this directly links fatty acid and sphingolipid biosynthesis. Further work will be required to find conditions appropriate for its formation and the role of the Trp37 in this conversion will be probed by site directed mutagenesis.

Conclusion

To begin a study of bacterial sphingolipid biosynthesis, we have isolated and purified recombinant proteins from the bacterium *S. wittichii*. Using various spectroscopic, kinetic and structural techniques we characterised SPT SW, and showed that it bind its co-factor PLP and its substrate L-serine. We proved that SPT SW was enzymatically active with L-serine and a range of long-chain acyl-CoA substrates. Furthermore we solved the high-resolution xray structure of the enzyme which allowed a structural comparison with the SPT from *S. paucimobilis*. We noted that despite high amino acid sequence identity the SPT isozymes displayed differences in kinetics and in structure. We found that the SPT gene resides alongside a putative small protein with sequence homology to bacterial Type II acyl carrier proteins and this led us to hypothesise that an ACP-thioester, rather than a CoAthioester may be the natural substrate for SPT. We co-expressed the *S. wittichii* ACP-SPT gene pair in *E. coli*, isolated the recombinant ACP and used mass spectrometry to show it was recovered in an apo-form. We investigated various PPTases in an effort to convert the ACP into its holo-form and acylated forms but succeeded in isolating only the holo-, C10, C12 and C14 acyl-forms. Analysis of the ACP primary sequence identified an unusual tryptophan residue next to the conserved

phosphopantetheinylation motif. Using *E. coli* ACP as a structural homolog, models of ACP SW were generated and suggest that this residue may block the attachment of longer acyl chains. Probing the role of this residue will be the focus of future structural and functional studies as will be the identification and characterisation of other downstream enzymes in the Sphingomonas sphingolioid biosynthetic pathway.

References

[1] Merrill, A. H. *J Biol Chem* 2002, 277, **25843-25846.**

[2] Futerman, A. H.; Hannun, Y. A. *EMBO reports* 2004, 5, **777-782.**

[3] Kobayashi, T.; Takahashi, M.; Nagatsuka, Y.; Hirabayashi, Y. *Biol Pharm Bull* 2006, 29, **1526-1531.**

[4] Hirabayashi, Y.; Igarashi, Y.; Merrill, A. H. J. *Sphingolipid Biology*; Springer-Verlag: Tokyo, 2006.

[5] Eliot, A. C.; Kirsch, J. F. *Annu Rev Biochem* 2004, 73**, 383-415.**

[6] Alexeev, D.; Alexeeva, M.; Baxter, R. L.; Campopiano, D. J.; Webster, S. P.; Sawyer, L. *J Mol Biol* 1998, 284, **401-419.**

[7] Webster, S. P.; Alexeev, D.; Campopiano, D. J.; Watt, R. M.; Alexeeva, M.; Sawyer, L.; Baxter, R. L. *Biochemistry* 2000, 39, **516-528.**

[8] Jordan, P. M.; Shemin, D. *In The Enzymes*; Boyer, P. D., Ed.; Academic Press: London, New York, 1972, p **339-356.**

[9] Ferreira, G. C.; Gong, J. *J Bioenerg Biomembr* 1995, 27, **151-159.**

[10] Astner, A.; Schulze, J. O.; van den Heuvel, J.; Jahn, D.; Schubert, W. D.; Heinz, D. W. *Embo J* 2005, 24, **3166-3177.**

[11] Schmidt, A.; Sivaraman, J.; Li, Y.; Larocque, R.; Barbosa, J. A. R. G.; Smith, C.; Matte, A.; Schrag, J. D.; Cygler, M. *Biochemistry* 2001, 40, **5151-5160.**

[12] Bashir, Q.; Rashid, N.; Akhtar, M. *Chem Commun* (Camb) 2006, **5065-5067.**

[13] Hanada, K. *Biochim Biophys Acta* 2003, 1632, **16-30.**

[14] Hanada, K.; Hara, T.; Fukasawa, M.; Yamaji, A.; Umeda, M.; Nishijima, M. *J Biol. Chem* 1998, 273, **33787-33794.**

[15] Han, G.; Gupta, S. D.; Gable, K.; Niranjanakumari, S.; Moitra, P.; Eichler, F.; Brown, R. H., Jr.; Harmon, J. M.; Dunn, T. M. *Proc Natl Acad Sci U S A* 2009, 106, **8186-8191.**

[16] Ikushiro, H.; Hayashi, H.; Kagamiyama, H. *J Biol Chem* 2001, 276, **18249-18256.**

[17] Ikushiro, H.; Hayashi, H.; Kagamiyama, H. *Biochim Biophys Acta* 2003, 1647, **116-120.**

[18] Ikushiro, H.; Hayashi, H.; Kagamiyama, H. *Biochemistry* 2004, 43, **1082-1092.**

[19] Ikushiro, H.; Islam, M. M.; Tojo, H.; Hayashi, H. *J Bacteriol* 2007, 189, **5749-5761.**

[20] Yard, B. A.; Carter, L. G.; Johnson, K. A.; Overton, I. M.; Dorward, M.; Liu, H.; McMahon, S. A.; Oke, M.; Puech, D.; Barton, G. J.; Naismith, J. H.; Campopiano, D. *J. J Mol Biol* 2007, 370, **870-886.**

[21] Raman, M. C.; Johnson, K. A.; Yard, B. A.; Lowther, J.; Carter, L. G.; Naismith, J. H.; Campopiano, D. *J. J Biol Chem* 2009, 284, **17328-17339.**

[22] Ikushiro, H.; Islam, M. M.; Okamoto, A.; Hoseki, J.; Murakawa, T.; Fujii, S.; Miyahara, I.; Hayashi, H. *J Biochem* 2009, 146, **549-562.**

[23] Shaner, R.; Allegood, J.; Park, H.; Wang, E.; Kelly, S.; Haynes, C.; Sullards, M.; Merrill, A. *J. J Lipid Res* 2009, 50, **1692-1707.**

[24] Wittich, R. M.; Wilkes, H.; Sinnwell, V.; Francke, W.; Fortnagel, P. *Appl Environ Microbiol* 1992, 58, **1005-1010.**

[25] Habe, H.; Ashikawa, Y.; Saiki, Y.; Yoshida, T.; Nojiri, H.; Omori, T. *FEMS Microbiol Lett* 2002, 211, **43-49.**

[26] White, S. W.; Zheng, J.; Zhang, Y. M.; *Rock. Annu Rev Biochem* 2005, 74, **791-831.**

[27] Lai, J. R.; Koglin, A.; Walsh, C. T. *Biochemistry* 2006, 45, **14869-14879.**

[28] Lambalot, R. H.; Gehring, A. M.; Flugel, R. S.; Zuber, P.; LaCelle, M.; Marahiel, M. A.; Reid, R.; Khosla, C.; Walsh, C. T. *Chem Biol* 1996, 3, **923-936.**

[29] Mercer, A. C.; Burkart, M. D. *Nat Prod Rep* 2007, 24, **750-773.**

[30] Weissman, K. J.; Muller, R. *Chembiochem* 2008, 9, **826-848.**

[31] Sanchez, C.; Du, L.; Edwards, D. J.; Toney, M. D.; Shen, B. *Chem Biol* 2001, 8, **725-738.**

[32] Quadri, L. E.; Weinreb, P. H.; Lei, M.; Nakano, M. M.; Zuber, P.; Walsh, C. T. *Biochemistry* 1998, 37, **1585-1595.**

[33] Cox, R. J.; Crosby, J.; Daltrop, O.; Glod, F.; Jarzabek, M. E.; Nicholson, T. P.; Reed, M.; Simpson, T. J.; Smith, L. H.; F., S.; Szafranska, A. E.; Westcott, J. *J Chem Soc, Perkin Trans* 1 2002, **1644-1649.**

[34] CCP4. *Acta Crystallographica Section D* 1994, 50, **760-763.**

[35] Kabsch, W. *J Appl Cryst* 1993, 26, **795-800.**

[36] Murshudov, G. N.; Vagin, A. A.; Dodson, E. J. *Acta Crystallogr D Biol Crystallogr* 1997, 53, **240-255.**

[37] LeDuc, R. D.; Taylor, G. K.; Kim, Y. B.; Januszyk, T. E.; Bynum, L. H.; Sola, J. V.; Garavelli, J. S.; Kelleher, N. L. *Nucleic Acids Res* 2004, 32, **W340-345.**

[38] Byers, D. M.; Gong, H. *Biochem Cell Biol* 2007, 85, **649-662.**

[39] Williams, R. D.; Wang, E.; Merrill, A. H., Jr. *Arch Biochem Biophys* 1984, 228, **282-291.**

[40] Jahan, N.; Potter, J. A.; Sheikh, M. A.; Botting, C. H.; Shirran, S. L.; Westwood, N. J.; Taylor, G. L. *J Mol Biol* 2009, 392, **763-773.**

[41] Kelly, R. C.; Bolitho, M. E.; Higgins, D. A.; Lu, W.; Ng, W. L.; Jeffrey, P. D.; Rabinowitz, J. D.; Semmelhack, M. F.; Hughson, F. M.; Bassler, B. L. *Nat Chem Biol* 2009, 5, **891-895.**

[42] Ploskon, E.; Arthur, C. J.; Evans, S. E.; Williams, C.; Crosby, J.; Simpson, T. J.; Crump, M. P. *J Biol Chem* 2008, 283, **518-528.**

[43] Garneau-Tsodikova, S.; Dorrestein, P. C.; Kelleher, N. L.; Walsh, C. T. J Am Chem Soc 2006, 128, **12600-12601.**

[44] Yin, J.; Straight, P. D.; McLoughlin, S. M.; Zhou, Z.; Lin, A. J.; Golan, D. E.; Kelleher, N. L.; Kolter, R.; Walsh, C. T. *Proc Natl Acad Sci U S A* 2005, 102, **15815-15820.**

[45] Gerber, R.; Lou, L.; Du, L. *J Am Chem Soc* 2009, 131, **3148–3149.**

[46] Cronan, J. E., Jr.; Klages, A. L. *Proc Natl Acad Sci U S A* 1981, 78, 5440-5444.

[47] Roujeinikova, A.; Simon, W. J.; Gilroy, J.; Rice, D. W.; Rafferty, J. B.; Slabas, A. R. *J Mol Biol* 2007, 365, **135-145.**

[48] Bates, P. A.; Sternberg, M. J. Proteins 1999, *Suppl* 3, **47-54.**

[49] Bates, P. A.; Kelley, L. A.; MacCallum, R. M.; Sternberg, M. *J. Proteins* 2001, Suppl 5, **39-46.**

[50] Contreras-Moreira, B.; Bates, P. A. *Bioinformatics* 2002, 18, **1141-1142.**

[51] Arnold, K.; Bordoli, L.; Kopp, J.; Schwede, T. *Bioinformatics* 2006, 22, **195-201.**

[52] Schwede, T.; Kopp, J.; Guex, N.; Peitsch, M. C. *Nucleic Acids Res* 2003, 31, **3381-3385.**

[53] Guex, N.; Peitsch, M. C. *Electrophoresis* 1997, 18, **2714-2723.**